High Performance Operation of Gain-Matched DFB Lasers

Nobuhiro NUNOYA, Monir MORSHED, Shigeo TAMURA and Shigehisa ARAI

Research Center for Quantum Effect Electronics, Tokyo Institute of Technology
2-12-1 O-okayama, Meguro-ku, Tokyo 152-8552, Japan
Phone: +81-3-5734-2512, Fax: +81-3-5734-2907, E-mail: aria@pe.titech.ac.jp

Abstract

High performance operation of GaInAsP/InP double-quantum-well gain-matched distributed feedback lasers fabricated by electron beam lithography, CH_4/H_2-riactive ion etching, and organo-metallic vapor-phase-epitaxial regrowth were successfully obtained. A record low threshold current density of 94 A/cm^2 and a record low threshold current of 7 mA among the 1.55 μm distributed feedback lasers were obtained for the 19.5-μm wide mesa-stripe and 2.3-μm wide buried heterostructure lasers, respectively. Moreover, single-mode operations of buried heterostructure DFB lasers were also realized due to gain matching effect.

1. Introduction

In order to realize high-density parallel optical interconnections, low threshold semiconductor lasers are indispensable[1]. High reflectivity mirrors and small active medium volume enable semiconductor lasers to operate with low threshold current, such as short-cavity edge-emitting lasers with high-reflection coatings[1] and vertical-cavity surface-emitting lasers (VCSELs)[2].

Distributed feedback (DFB) and distributed Bragg reflector (DBR) lasers[3] with deep corrugations have similar advantages, especially a DFB laser with deeply etched wirelike active regions which can be realized by adopting a strongly anisotropic etching feature of a dry etching. A fabrication method combining a dry etching and a regrowth has been used for complex-coupled DFB lasers[4] and quantum-wire and quantum-box lasers[5-7]. In previous work, we fabricated DFB lasers consisting of deeply etched wirelike active regions with 1%-compressively strained (CS) 5-quantum-wells (5QWs). A low threshold current (I_{th}) of 20 mA and a low threshold current density (J_{th}) of 330 A/cm^2 were reported[8].

In this paper, we would like to report further reduction of the threshold current density and the threshold current by means of reducing the volume of the active region, *i.e.*, reductions of the number of quantum-wells and the active region width.

2. Threshold Current Analysis

In order to design the cavity structure appropriate for an ultra-low threshold current operation, threshold current dependences on the number of quantum-wells and the width of the wirelike active regions were calculated using a model shown in Fig. 1. An index-coupling coefficient (κ_i) can be expressed as[9]

$$\kappa_i = \frac{\sqrt{2}}{\lambda}\Delta n \sin\left(\frac{\pi W}{\Lambda}\right), \qquad (1)$$

where the Δn, W, and Λ denote a difference of equivalent refractive index of deep corrugations, the width of the active region, and the period of the corrugation, respectively. In order to derive Eq. (1), the first order component in the Fourier series was considered for the longitudinal distributions of the refractive index.

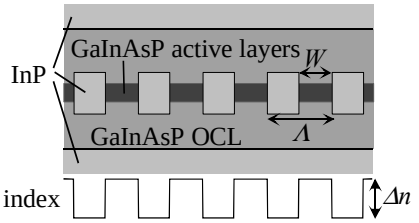

Figure 1 Calculation model of DFB laser with deeply etched active regions.

Figure 2 shows theoretical threshold current dependences on (a) the wire width (W) and the number of QWs, respectively, of DFB lasers with the stripe width (W_s) of 1 μm and the corrugation period (Λ) of 240 nm. In these calculations, only an index-coupling was considered because the index-coupling coefficient is much stronger than the gain-coupling coefficient and facet reflections were neglected. The maximum index-coupling coefficient is calculated to be 390 cm^{-1} for W/Λ of 0.5 and Δn of 0.03 from Eq. (1).

As can be seen in Fig. 2(a), the lowest threshold current can be obtained at W/Λ = 0.35 and the cavity length of around L = 300 μm for 5QWs-DFB lasers because of a volume effect and a high index-coupling, while the index-coupling coefficient is the largest at W/Λ = 0.5. Figure 2(b) shows the threshold current dependence on the cavity length of single QW (SQW), double QWs (2QWs), and 5QWs-DFB lasers with an optimal active region width for a low threshold current operation. In cases of SQW and 2QWs-DFB lasers, threshold current reduction due to a volume effect

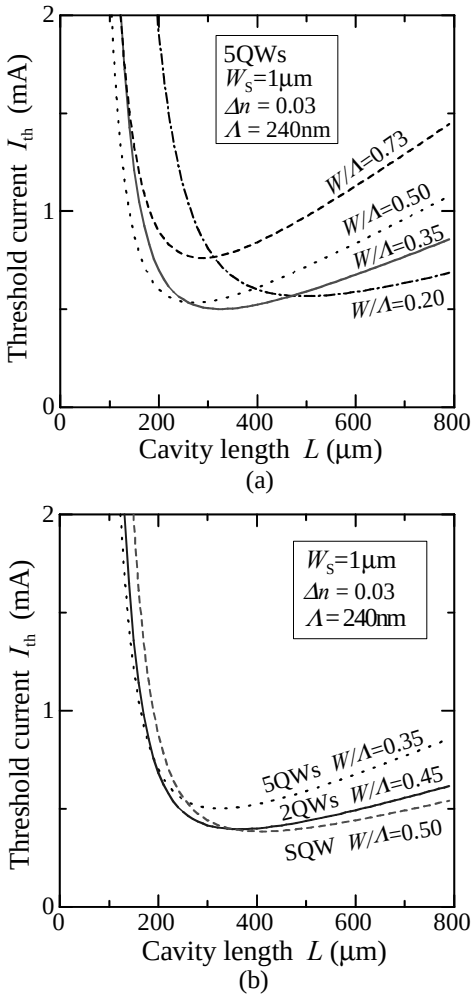

Figure 2 Threshold current dependence on the cavity length for (a) various wire width of 5QWs-DFB laser, and (b) almost optimal conditions of the number of QWs and the wire width.

diminishes because of the reduction of κ_i. The threshold current of less than 0.5 mA can be obtained for single- and double-quantum-wells with an in-plane space filling factor of $W/\Lambda \sim 0.50$.

3. Experimental Results

3.1 Mesa stripe DFB lasers

To compare with 5QWs DFB lasers reported in previous work and to study the wire width dependence of threshold current, four kinds of DFB lasers with different wire width (W) of 65 nm (W/Λ=0.27), 83 nm (0.35), 115 nm (0.48), and 145 nm (0.60), were fabricated on the same wafer with a fixed corrugation period (Λ) of 240 nm[10]. A 1%-CS 2QWs structure on p-InP (100) substrate was used as an initial wafer. Deeply etched corrugations with a period of 240 nm in the active region were formed by CH_4/H_2 reactive ion etching (RIE) and organo-metallic vapor phase epitaxy (OMVPE). CH_4/H_2-RIE and O_2 ashing to remove the polymer deposited during the RIE were repeated several times to obtain a vertical shape. Wet chemical etchings were carried out before the OMVPE regrowth. In the regrowth process, when the groove region was regrown, relatively slow growth speed of 250 nm/h and a low

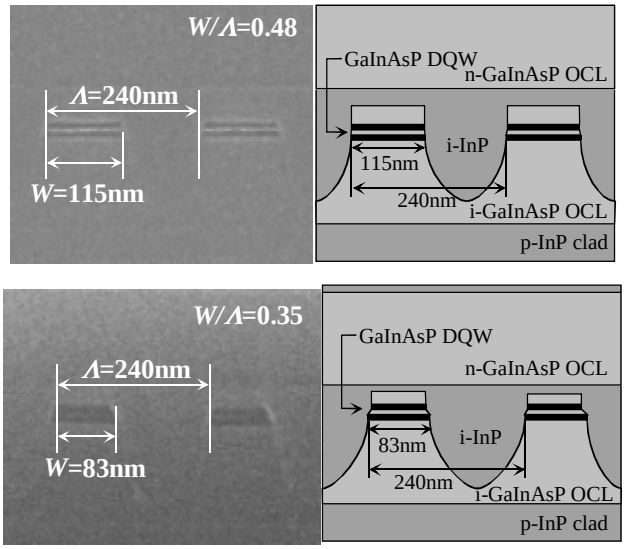

Figure 3 Cross sectional SEM views (Examples for W/Λ=0.48 and 0.35)

growth temperature of 600 °C were used to obtain a flat surface and low damage interfaces, although 1.2 μm/h and 650 °C were used in the growth of initial MQWs wafers. Finally, mesa stripe lasers (W_s=19.5 μm) were formed by a conventional photolithography and a wet etching. Cross sectional SEM views of examples for W/Λ of 0.48 and 0.35 are shown in Fig. 3. The index-coupling coefficients for W/Λ=0.27, 0.35, 0.48 and 0.60 were calculated to be 280 cm^{-1}, 335 cm^{-1}, 360 cm^{-1} and 340 cm^{-1}, respectively, from each structure by Eq. (1).

Figure 4 shows light output (I-L) characteristics of 3 samples under a pulsed condition, for examples, where the lowest threshold current I_{th}=7 mA was obtained for a cavity length of 280 μm and W/Λ=0.35, and the lowest threshold current density J_{th}=94 A/cm^2 for L=600 μm and W/Λ=0.48. To our knowledge, this value is the lowest among 1.55 μm DFB lasers ever reported. The threshold current of 2QWs-DFB lasers was markedly reduced in comparison with that of 5QWs-DFB lasers (I_{th}=20 mA)[8], which is attributed to the smaller active

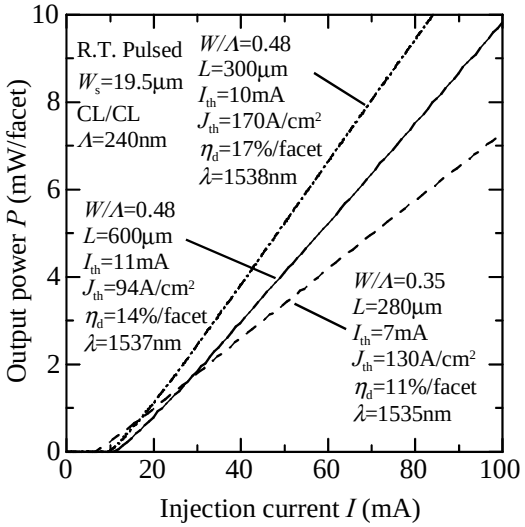

Figure 4 I-L characteristics of 2QWs-DFB lasers which showed lowest I_{th}, lowest J_{th} and high η_d.

region volume and higher index-coupling coefficient κ_i. An external differential quantum efficiency (η_d) of 10~15 %/facet was typically obtained. The highest η_d was 17 %/facet for L=300 μm and W/Λ = 0.48.

The index-coupling coefficient κ_i was estimated from a measurement of the stop-band width. A stop-band width is observed to be about 8 nm in case of W/Λ=0.48 and L=740 μm. By means of the estimation of the index-coupling coefficient from the stop-band width of DFB lasers with various wire width, the wire width dependence of the index-coupling coefficient was obtained as shown in Fig. 5. The solid line indicates the calculation for Δn=0.028, which is the difference of equivalent refractive indexes estimated from the cross sectional structure of a DFB laser with W/Λ=0.48. As can be seen, measurement results are in good agreement with the theoretical curve. As a consequence, it was confirmed experimentally that the index-coupling coefficient could be designed easily on the same wafer by means of varying the in-plane space-filling factor W/Λ.

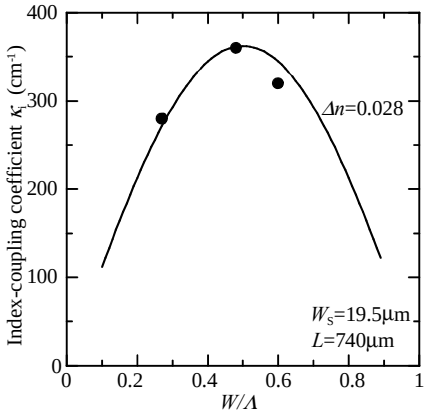

Figure 5 Wire width dependence of Index coupling coefficient. The solid line is calculation result for Δn=0.028 in Eq. (1).

Figure 6 shows the threshold current dependence on a cavity length of 4 kinds of DFB lasers. As can be seen, threshold current density between 94 A/cm^2 and 130 A/cm^2 was obtained for samples with W/Λ=0.35 and W/Λ=0.48, while that for W/Λ=0.27 and 0.60 was slightly higher due to poor optical confinement and larger volume of the active region, respectively. The lowest threshold current would be obtained for DFB lasers with the cavity length of around 300 μm as predicted by theoretical results shown in Fig. 2(b).

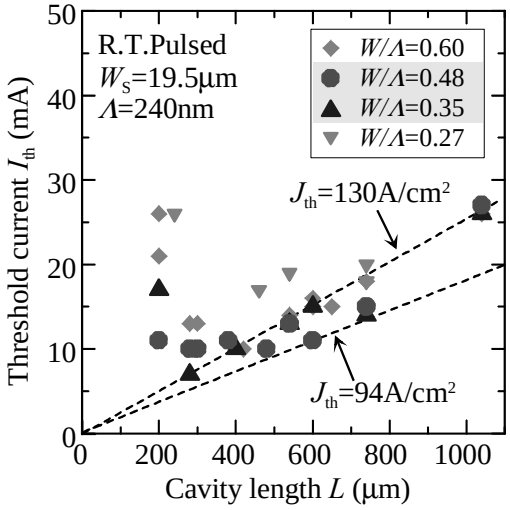

Figure 6 Cavity length dependence of the threshold current for 2QWs-DFB lasers with various wire widths

Although figures aren't shown in this paper, even lower threshold current of 5.8 mA was achieved for a 15-μm wide stripe DFB laser (J_{th}=176 A/cm^2 @ W/Λ=0.35, L=220 μm) due to the reduction of active volume.

3.2 Buried Heterostructure DFB lasers

To reduce the threshold current, we fabricated buried heterostructure (BH) DFB laser with wirelike active regions[11]. For BH-2QWs-DFB lasers, we used 1%-CS-2QWs with tensile strained barrier layers on a p-InP substrate (partially strain compensated wafer) in order to reduce fabrication damages at etched/regrown interfaces[7]. Figure 7 shows an illustration of BH-DFB laser structure and its cross-sectional SEM views of deep corrugations and the BH stripe region. The stripe width and the wire width of the grating were 2.3 μm and 90 nm (W/Λ=0.38), respectively. The index-coupling coefficient was estimated to be 390 cm^{-1} from the structure.

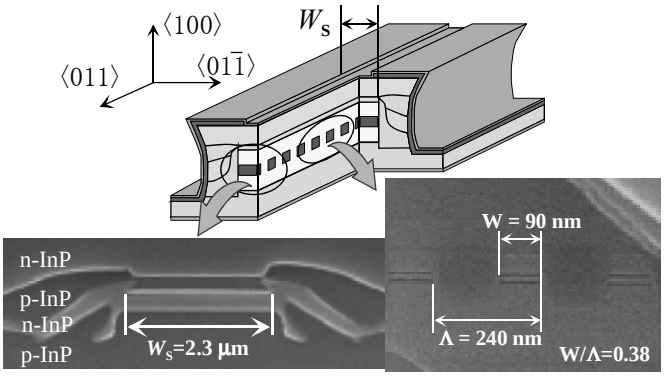

Figure 7 Schema of BH-2QWs-DFB laser and its cross sectional SEM views.

Submilliampere operations were successfully obtained for cavity length below 240 μm under room temperature continuous-wave (RT. CW). Figure 8 shows typical *I-L* characteristic of three samples of submilliampere operating BH-DFB lasers. Threshold current as low as 0.7 mA was obtained for the cavity length of 200 μm (R.T. CW). To our knowledge, this is the lowest value in the 1.55 μm wavelength DFB laser. Threshold current density was calculated to be 150 A/cm^2. The external differential quantum efficiency η_d was 23 %/facet. And quite good reproducibility was also observed though samples had both cleaved facets.

Figure 9 shows an emission spectrum of BH-DFB laser at a bias current of 1.1 mA, whose threshold current was 0.9 mA (L=240 μm, η_d=22 %/facet). While some modes can be seen at both sides of the stopband, the nearest long-wavelength mode to the stopband oscillated lasing modes for all measured samples were

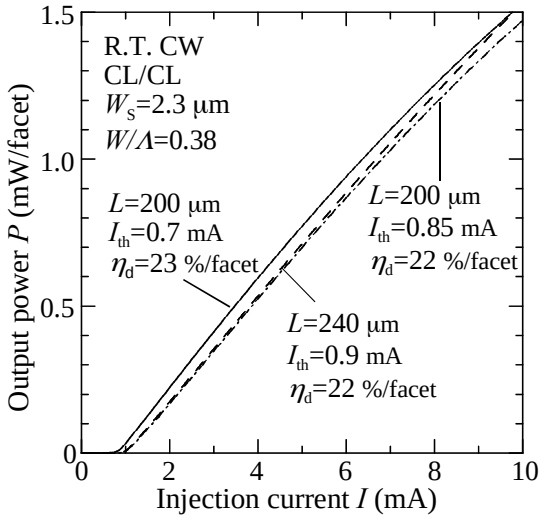

Fig. 8 I-L characteristics of three samples

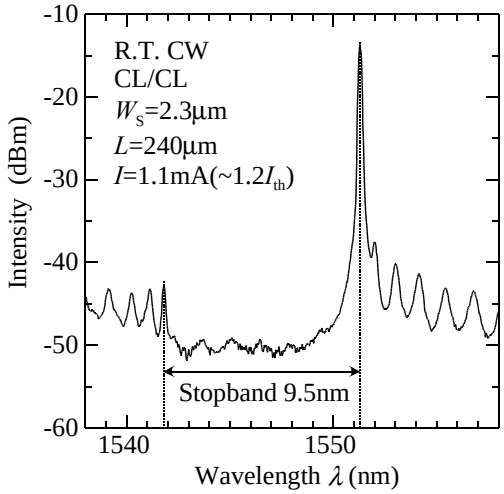

Fig. 9 Emission spectrum of a DFB laser at bias current of 1.1mA (1.2I_{th}).

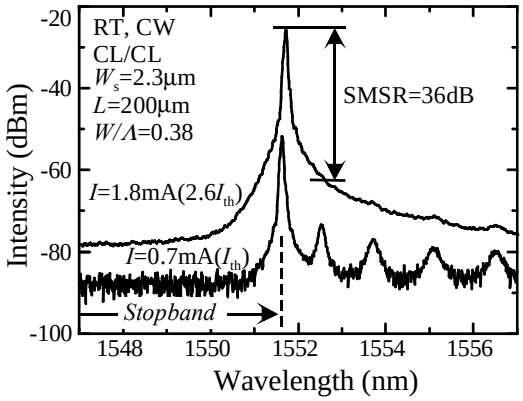

Fig. 10 Emission spectra of BH-DFB laser at the long wavelength side of stopband.

observed at long-wavelength side of the stopband. In case of in-phase grating, which means that a phase of index grating is the same as that of gain grating, standing wave profiles of long-wavelength side modes match gain regions greater than that of short-wavelength side modes[12], which is called a gain matching effect. We believe this is the reason why the lasing mode of all samples measured was observed at long-wavelength side of the stopband. The index-coupling coefficient was estimated to be 390 cm^{-1} from the stopband width of 9.5 nm. From the spectrum of the other DFB laser for L of 200 μm shown in Fig.10, sub-mode suppression ratio (SMSR) of 36 dB at a bias current of 2.6I_{th} (I_{th}=0.7 mA) was obtained.

5. Conclusion

In conclusion, the active volume and wire width dependence of threshold current of 1.55 μm wavelength DFB lasers with deeply etched wirelike active regions was investigated both theoretically and experimentally. As the result, a record low threshold current density of 94 A/cm^2 was achieved for 2QWs DFB laser with the cavity length of 600 μm. Furthermore, we successfully obtained a record low threshold current of 0.7 mA for BH-2QWs-DFB laser. Submilliampere and single-mode operations were realized.

Acknowledgment

The authors would like to thank Prof. Emeritus Y. Suematsu, Prof. K. Iga, Prof. K. Furuya, Prof. M. Asada, Prof. F. Koyama, Assoc. Prof. Y. Miyamoto, Assoc. Prof. M. Watanabe and Assoc. Prof. T. Miyamoto of Tokyo Institute of Technology for fruitful discussions. This research was financially supported by "Research for the Future Program (#JSPS-RFTF96P00101) of The Japan Society for the Promotion of Science and a Grant-In-Aid for a Scientific Research Project in a Priority Area "Single Electron Nano-Electronics" and Fundamental Research B (#10450115 and #12555098) from the Ministry of Education, Science, Sports and Culture, Japan.

References

[1] K. Uomi, T. Tsuchiya, M. Komori, A. Oka, T. Kawano, and A. Oishi: IEEE J. Select. Top. Quantum Electron., Vol. 1, No. 2, pp.203-210, 1995.

[2] N. M. Margalit, D. I. Babic, K. Streubel, R. P. Mirin, R. L. Naone, J. E. Bowers and E. L. Hu: Electron. Lett., Vol. 32, No. 18, pp. 1675-1677, 1996.

[3] M.M. Raj, J. Wiedmann, Y. Saka, H. Yasumoto and S. Arai: Electron. Lett., Vol. 35, No. 16, pp. 1335-1337, 1999.

[4] A. Talneau, N. Bouadma, Y. Lebellego, S. Slempkes, A. Ougazzaden, G. Patriarche and B. Sermage: IEEE Photon. Technol. Lett., Vol. 10, No. 8, pp. 1070-1072, 1998.

[5] U. A. Griesinger, S. Kronmüller, M. Geiger, D. Ottenwälder, F. Scholz and H. Schweizer: J. Vac. Sci. Technol., Vol. B14, No. 6, pp. 4058-4061, 1996.

[6] N. Nunoya, M. Nakamura, H. Yasumoto, S. Tamura and S. Arai: Jpn. J. Appl. Phys. Vol. 39, Part 1, No. 6A, pp. 3410-3415, 2000.

[7] N. Nunoya, H. Yasumoto, H. Midorikawa, S. Tamura and S. Arai: Jpn. J. Appl. Phys. Vol. 39, Part 2, No. 10B, pp. L1042-L1045, 2000.

[8] N. Nunoya, M. Nakamura, H. Yasumoto, S. Tamura and S. Arai: Jpn. J. Appl. Phys., Vol. 38, Part 2, No. 11B, pp. L1323-L1326, 1999.

[9] K. Kudo, S. Arai, and K. C. Shin: IEEE Photon. Technol. Lett., Vol. 6, No. 4, pp. 482-485, 1994.

[10] M. Nakamura, N, Nunoya, H. Yasumoto, M. Morshed, K, Fukuda, S. Tamura and S. Arai: Electron. Lett., Vol. 36, No. 7, pp.639-640, 2000.

[11] N. Nunoya, M. Nakamura, H. Yasumoto, M. Morshed, K. Fukuda, S. Tamura, and S. Arai: Electron. Lett., Vol.36, No. 14, pp. 1213-1214, 2000.

[12] A. Champagne, R. Maciejko, D. M. Adams, G. Pakulski, B. Takasaki, and T. Makino: IEEE J. Quantum. Electron., Vol. 35, No. 10, pp. 1390-1401, 2000.